

Extended Kalman filtering for vortex systems. Part II: Rankine vortices and observing-system design

Kayo Ide ^{*}, Michael Ghil

Department of Atmospheric Sciences and Institute of Geophysics and Planetary Physics, University of California, Los Angeles, CA 90095-1565, USA

Received 13 February 1996; revised 18 July 1996; accepted 18 July 1996

Abstract

Point-vortex systems with both regular and chaotic motion can be tracked by a combination of Lagrangian observations of vortex position and of Eulerian observations of fluid velocity at a few fixed points. If only Eulerian observations are available, singularities in the tracking can develop due to nonlinearity in the observing functions on two occasions: when point vortices pass very close to an observing station, and when the observed speed is small. In Part II of this two-part paper, the vorticity concentrations are approximated by Rankine vortices with finite core in solid-body rotation, while a cut-off criterion is imposed on the Eulerian observations; this removes the singularities and hence results in satisfactory tracking when the observations are judiciously chosen.

The main result is that a number of observations comparable to that of the distinct vorticity concentrations suffices for very accurate tracking. The key elements for successful tracking of Rankine-vortex systems using nonlinear, Eulerian observations are: distribution of available stations, threshold criteria for the selection of stations used in each update, and the observing frequency. Simple analysis provides the optimal estimate for these key elements, together with the optimal size of the estimated Rankine vortices. © 1997 Elsevier Science B.V.

1. Introduction

Geophysical fluid dynamicists have used data assimilation to describe the motion of the atmosphere and oceans from incomplete and noisy data (Ghil, 1989, Daley, 1991,

^{*} Corresponding author.

Panel on Model-Assimilated Data Sets for Atmospheric and Oceanic Research, 1991, Ghil and Malanotte-Rizzoli, 1991). Kalman filtering and its nonlinear extension, extended Kalman filtering (EKF), are advanced data-assimilation methods rooted in sequential estimation theory (Kalman, 1960; Kalman and Bucy, 1961; Jazwinski, 1970; Ghil et al., 1981). They allow us to forecast and estimate the variables of interest by combining dynamical and statistical aspects of the system. In meteorology and oceanography, data assimilation has been applied to help understand the fundamental physics and dynamics of the flow or for the practical purposes of numerical prediction (Bengtsson et al., 1981; Wunsch, 1988; Robinson et al., 1989; Ghil and Malanotte-Rizzoli, 1991).

To describe the dynamical aspects of geophysical fluids, most studies so far used an Eulerian framework, independent of the goals and techniques of the data-assimilation process. In this framework, fluid quantities such as velocity and density are computed on a spatial or spectral grid according to a finite-dimensional dynamical system of ordinary differential equations obtained by discretizing an infinite-dimensional system of partial differential equations, such as the primitive equations or the quasi-geostrophic equations which describe the flow fields of interest. However, the atmosphere (McWilliams, 1980) as well as the ocean (Robinson, 1983) are known to have much of their energy and vorticity concentrated in approximately two-dimensional localized coherent structures, rather than having a spatially near-homogeneous distribution of fluid quantities (McWilliams, 1991). In Part I of this study (Ide and Ghil, 1997a), we saw that, using a Lagrangian representation of the flow field in terms of point vortices, a number of observations comparable to that of vortices suffices, in general, to estimate well the entire flow field.

Besides the dynamics of the flow, that may be represented better by a Lagrangian description, the observations used are another important aspect of data assimilation. Observations can be Lagrangian, e.g. buoy trajectories (Carter, 1989) or sea-surface height contours based on remote sensing (Mariano, 1990), as well as Eulerian, such as temperature or current measurements at a fixed station. Therefore geophysical data assimilation may need to deal with Lagrangian dynamics combined with either Lagrangian or Eulerian data sets, or with some combination of both. Based on knowledge about the underlying flow dynamics and possible observations on it, one can design an observing system that provides efficient and successful estimation. Observing-system optimization (Ghil and Ide, 1994) is critical for the oceans where each data point counts, due to the limited number of observations. Barth and Wunsch (1990) and Barth (1992) considered specific optimization problems for acoustic tomography data in linear ocean models (steady-state and time-dependent, respectively) using simulated annealing. Bennett (1992) also considered, in fairly general terms, the problem of observing-system, or 'antenna' design for ocean models.

In order to estimate the large-scale flow patterns of geophysical or planetary flows, we used the EKF on point-vortex system in Part I. The EKF consists of the sequential application of two steps (Gelb, 1974, Ghil, 1989, Miller et al., 1994): in the first step, the state variables and their expected error-covariance matrix are forecast from one observing time to the next, according to the underlying dynamics of the system; in the second step, an update of model variables at observing time combines forecast and

observations so as to minimize the estimated error in a least-square sense. In this two-part paper, we focus on observing-system design, and hence emphasize the second step. Ide and Ghil (1997b) discuss a number of issues concerning the first step.

Our numerical and analytical results in Part I showed that, despite the possible complex motion of point-vortex systems (Aref, 1984), the EKF works well when all the vortex positions are observed, albeit with relatively large errors. EKF tracking may, however, fail when the number of vortex-position data is insufficient and they are replaced entirely or partially by velocity observations at given locations. There are two main causes of unsuccessful EKF performance when station-velocity observations are used: (1) when at least one of the vortices is very close to the station, so that the measured velocity is very large; (2) when the magnitude of the measured velocity is almost zero, either near a stagnation point where induced velocities due to all the vortices present cancel out or when all the vortices are far away from the station.

There are simple, but crude remedies for both problems. In order to avoid the second one, a cut-off criterion for the minimum velocity can be imposed. To avoid the velocity singularity due to the close approach of the vortices to the stations, a maximum velocity cut-off criterion could be imposed as well. At each update time, stations for which either the observed velocity or the one reconstructed from the estimated vortex positions do not meet either cut-off criterion can be ignored in the update process. These criteria were implemented for the point-vortex systems of Part I (not shown there); they do help avoid poor EKF performance in a variety of situations. But the latter type of cut-off can also have deleterious effects, since velocity updates perform best when the vortices are close to the station used in the update—as shown analytically in Part I.

In order to overcome the difficulties encountered with point-vortex systems at a more fundamental level, we approximate in Part II the flow field using Rankine vortices. A Rankine vortex is a finite-core circular vortex with top-hat vorticity distribution. The velocity inside the core is a linear function of distance from the center of the vortex, while the outside velocity field decays like that of a point vortex (e.g. Ghil and Solan, 1973). As the core radius goes to zero while keeping the total circulation constant, a Rankine vortex becomes a point vortex. As long as all vortices are well separated, the centers of the Rankine vortices move as if they were point vortices with the same circulation, while the singularities associated with the latter area removed from the flow field. Although this is a crude approximation, it is realistic in the sense that it captures the main interaction between localized coherent vorticity structures, as well as representing the local velocity field around each vortex more realistically than a point vortex does (e.g. Olson, 1980, Feliks and Ghil, 1996). When the minimum cut-off criterion is properly imposed on the Rankine-vortex system, numerical and analytical results show that tracking using only nonlinear Eulerian observation can be successful as well as reasonably efficient.

Throughout this study, the total circulation and core radius of the Rankine vortices are assumed to be known. These values can be also estimated, along with the evolution of the vortices, by treating the vortex-system tracking as a parameter-identification problem (Ide and Ghil, 1995).

Part II of this paper is organized as follows: in Section 2 we introduce the Rankine-vortex model and the corresponding EKF formulation. In Section 3 numerical

results using the nonlinear Eulerian data only are shown; in Section 4 we give a brief analysis for the optimization of the observing system and point out the key elements in successful tracking for the Rankine-vortex system. Analytical and numerical results are summarized and discussed in Section 5. The notation used here follows Ide et al. (1997).

2. Model formulation

In the absence of other vortices, a steady Rankine vortex (Fig. 1) is an exact, axisymmetric solution of the Euler equations for two-dimensional flow. A Rankine vortex whose core area is $\pi\sigma^2$ and total circulation is Γ undergoes solid-body rotation of angular velocity $\Gamma/2\pi\sigma^2$, without deforming nor changing its position; it induces the same outside flow field as a point vortex of circulation Γ located at the center of the Rankine vortex. The velocity field of the Rankine vortex whose center is located at the origin of the coordinate system is

$$\frac{dz^*}{dt} = \begin{cases} \frac{\Gamma}{i2\pi\sigma^2} z^*, & \text{for } |z| \leq \sigma, \\ \frac{\Gamma}{i2\pi z}, & \text{for } |z| > \sigma, \end{cases} \quad (1)$$

where $z = x + iy$ is the complex coordinate and z^* is its complex conjugate. The velocity field is rotational inside the core and irrotational outside of it. The radial velocity u_r is identical to zero, while the azimuthal velocity u_θ is linear in z inside the core and decays like $1/r$ outside, where r is the distance from the center. The velocity is continuous at the core boundary $r = \sigma$, although its spatial derivatives are discontinuous there due to the vorticity discontinuity (see Fig. 1).

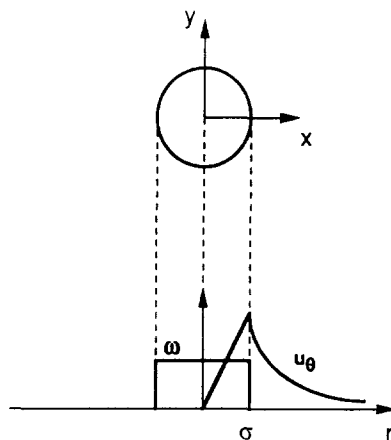


Fig. 1. Rankine vortex: plan view and, below, vorticity distribution ω and azimuthal velocity field u_θ in a cross-section.

When there is more than one vortex in the flow field, nonlinear interaction among them results in translation of vortex centers together with deformation of the vortex configuration around the center (Ide and Ghil, 1997c). For isolated vortices, i.e. $\sigma/l \ll 1$ where l is the distance between vortices, translation of the centers without changing vortex configuration is a good approximation of vortex interaction. We shall use a Rankine-vortex method of describing the evolution of the flow field, based on isolated Rankine vortices advected without deformation. In this description, the vortices move as if they were point vortices, while the singularities in the velocity field are removed. A flow field with N Rankine vortices is completely determined by N center positions $\{z_{v,l}; l = 1, \dots, N\}$, with subscript ‘v’ for ‘vortex’, when core radius σ_l and total circulation Γ_l of each vortex are prescribed.

This approximate description will obviously break down in the long run, as vortices approach each other, deform strongly, and trap or repel each other (e.g. McWilliams, 1991). Data assimilation, however, is concerned with short-term, rather than asymptotic, behavior of the system, and the Rankine-vortex method is clearly an improvement on the point-vortex method. A more detailed treatment of close-range interaction between vortices is being pursued by a moment model (Ide and Ghil, 1997c).

Using the Rankine-vortex method, we reformulated the EKF for point vortices of Part I; the same notational conventions are followed. The EKF consists of the successive application of two steps, forecast and update. The state variables, i.e. vortex-center positions, and corresponding equations of motion for the Rankine-vortex method are the same as for the point-vortex method; hence the forecast step of the EKF here is equivalent to that for point vortices. The forecast of vortex positions and the error-covariance matrix are computed according to Eq. (3) in Part I; the numerical implementation is also the same.

For the update, we first define the observations in the Rankine-vortex system. In the present paper, we use two types of observations (as we did in Part I), i.e. vortex-center positions $\mathbf{c}^o = \{c_1^o, \dots, c_{M_v}^o\}$ and station-velocity data $\mathbf{u}^o = \{u_1^o, \dots, u_{M_s}^o\}$, where subscript ‘s’ denotes ‘station’ and M_v and M_s are the number of corresponding observations. Possible ways of implementing such measurements in oceanographic practice were mentioned in Section 2.2 there. The velocity observations now have the form:

$$\mathbf{u}^o = \{u_1^o, u_2^o, \dots, u_{M_s}^o\}, \tag{2a}$$

where

$$u_k^o = h_{s,k}(z_v^l, z_{s,m}) + w_{s,k}^l, \tag{2b}$$

$$h_{s,k} = \sum_{n=1}^N h_{s,kn}, \tag{2c}$$

$$h_{s,kn} = \begin{cases} \frac{\Gamma}{i2\pi\sigma_n^2} (z_{s,m} - z_{v,n})^*, & \text{for } |z_{s,m} - z_{v,n}| \leq \sigma_n, \\ \frac{\Gamma}{i2\pi(z_{s,m} - z_{v,n})}, & \text{for } |z_{s,m} - z_{v,n}| > \sigma_n; \end{cases} \tag{2d}$$

here superscripts ‘o’ and ‘t’ stand for ‘observation’ and the ‘true’ system, $z_{s,m}$ is the station where u_k^o is observed, and the subscript that represents the observation time has been dropped for convenience. When the vortex n is within distance σ_n of station m , the velocity observation $h_{s,kn}$ is a linear function of $z_{v,n}$. The update using velocity observations is thus expected to perform much better when a vortex is close to a station than for a point vortex (cf. Part I). The error characteristics of the velocity observations are as described in Section 3.1 of Part I.

Use of the Rankine-vortex method takes care automatically of the problem caused by the singular nature of the point-vortex velocity field, by removing the singularity. To deal with the second problem noticed in Part I when using velocity observations, i.e. that of (very) small observed velocities (see Section 1 here), we impose a minimum-velocity cut-off criterion. In Rankine-vortex systems, there are mainly three occasions when velocity at a station is small: (i) all the vortices are far away from the station; (ii) no vortices are in the immediate neighborhood of the station and the sum of induced velocities at the station (almost) cancels; and (iii) one of the vortices is very close to the station and the sum of velocities induced by the other $N - 1$ vortices is very small due to reasons (i) or (ii) above. Hence, to take advantage of the linearity of the station observation functions in the Rankine-vortex system, we impose a minimum velocity criterion $|dz/dt| \geq u_{\min}$ but only in case (i) or (ii), i.e. if there are no estimated or observed vortices in the immediate neighborhood of the station. A vortex is considered to be in the immediate neighborhood of a station if the distance between the two is smaller than the corresponding Rankine-core radius.

In the present paper, we deal only with the more realistic situation of systems subject to stochastic forcing. Indeed, we saw in Part I (cf. also Miller et al., 1994) that absence of stochastic forcing tends to yield insufficient gain (whether the underlying system undergoes regular or irregular motion) and hence the update does not have sufficient impact after an initial adjustment interval. Stochastic forcing in vortex systems is equivalent to forcing of the large-scale, coherent structures by the smaller-scale motions; this is the case independently of whether the description is at the level of point vortices (Part I), Rankine vortices (here), or more sophisticated vortex models (Ide and Ghil, 1997c).

3. Numerical results

In this section, we present numerical results on EKF performance for systems with four and six Rankine vortices subject to stochastic forcing. In the presence of stochastic forcing, the number of vortices is not as important a factor for EKF performance, although systems with a larger number of vortices may require a larger number of observations for successful tracking; as seen numerically and analytically in this section and the next, this number does still not need to exceed, on average, that of vortices. Key factors in EKF performance are: (1) the effects of using Rankine vortices as compared with point vortices; (2) the statistics of all the available observing stations; (3) the statistics of the ‘active stations’ at each update; and (4) the update frequency. By ‘available stations’ we mean all the stations that can provide velocity observations at a

given update time. Among the available stations, only those who meet the cut-off criteria are active in each update. Screening criteria, by distance between the station where a flow quantity is observed and the (Eulerian) grid point where a model variable is to be updated, are also used in the optimal interpolation (OI) method of data assimilation that is applied operationally by all major numerical weather prediction centers (Daley, 1991, Ghil and Malanotte-Rizzoli, 1991).

The numerical results are presented in terms of the most informative quantities. The trace and components of the error-covariance matrix \mathbf{P} give a least mean-square indicator of EKF performance. Time histories of estimated, observed, and true vortex motion (x_v and y_v versus time) show how well the EKF actually tracks the true system. Comparison between the evolution of the actual vortex motion and the corresponding components of \mathbf{P} provides overall performance of the EKF. The number of stations active for each update indicates the efficiency of the update process. In order to see how well the (Eulerian) velocity field is reconstructed from the (Lagrangian) vortex-system dynamics, we also present the evolution of the magnitude of the velocity measured at the station placed at the origin (0, 0). In each figure, solid curves, open diamonds, and plus marks correspond to the estimated, true, and observed values, respectively, and true and observed values are plotted only every 5 time units for presentation purposes, unless otherwise noted.

In each assimilation run presented here, the vortices are initially located at positions that are slightly perturbed from an even distribution along a unit circle centered at (0, 0); this would provide chaotic trajectories for four or more point vortices even in the absence of stochastic forcing (see Part I). The Rankine vortices are all set to have core radius $\sigma = 0.1$ and total circulation $\Gamma = 1$. The system is updated every 0.1 time unit, using velocity observations only; this is more frequent than for successful tracking with all four vortex-position observations in Part I. Available stations are placed on a 1.5×1.5 grid to cover the basic square region $\mathcal{R} = \{-3 \leq x \leq 3, -3 \leq y \leq 3\}$ uniformly; this is where the vortices are expected to spend most of the time. Station velocities are the only type of observations used, unless otherwise noted. The cut-off threshold u_{\min} defined in Section 2 is chosen so as to demonstrate various aspects of both successful and unsuccessful data assimilation: $u_{\min} = 0.40$ for Figs. 3 and 6, $u_{\min} = 0.53$ for Figs. 5 and 7, and no cut-off criterion is imposed for Fig. 2. Initial data and set-up for \mathbf{P} , \mathbf{Q} , and \mathbf{R} are the same as in Part I. The choice of u_{\min} will be discussed in Section 4 as part of observing-system design.

We start from a typical case of unsuccessful EKF performance while using the point-vortex method to recall the possible problems that arise when nonlinear Eulerian observations are used for point vortices. No cut-off is imposed and hence all velocity observations at the $5 \times 5 = 25$ stations are active in each update. At $t \sim 10$, the update fails to estimate the motion of the system properly, due to small observed velocities, and Vortex 3 drifts away from its true trajectory. The trace and corresponding component of the error-covariance matrix \mathbf{P} do alert us to the loss of tracking by their rapid growth (Fig. 2(a) and (b)).

In general, when the components of \mathbf{P} increase, the weights for updating become larger, so as to pull the system back towards a state that would provide estimated values of the observed velocities similar to those actually observed. In this experiment, the

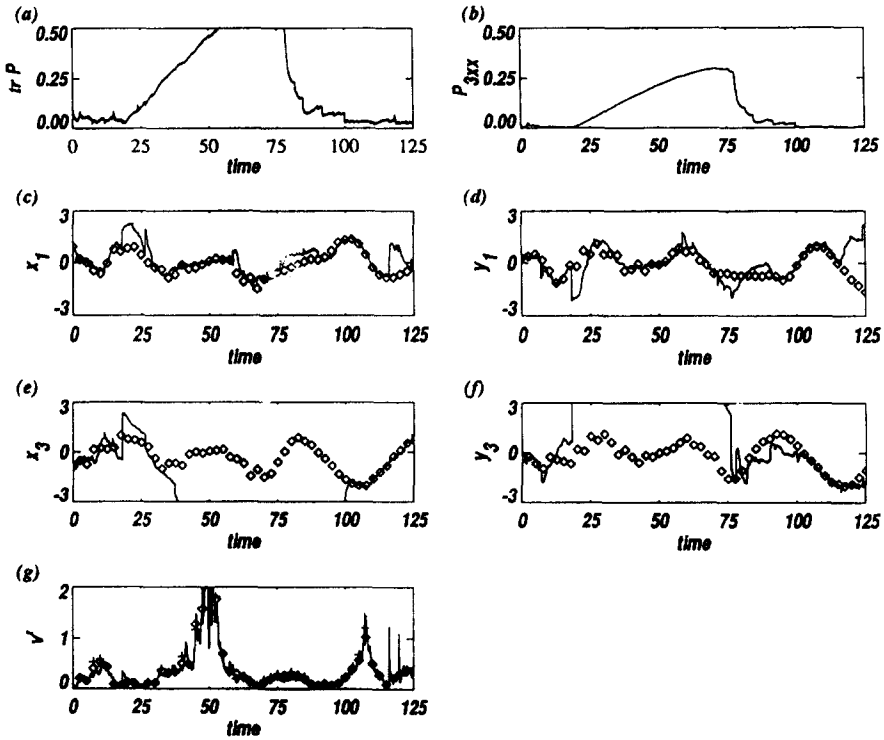


Fig. 2. The performance of the EKF for four point vortices with stochastic forcing, when station velocities are observed every 0.1 time units and no cut-off criterion is imposed: (a) $tr\mathbf{P}$; (b) P_{3xx} ; (c) x_1 ; (d) y_1 ; (e) x_3 ; (f) y_3 ; and (g) square of velocity at $(0, 0)$.

estimated position of Vortex 3 drifts out of the basic region \mathcal{R} and hence far away from any available station (Fig. 2(e) and (f)). The corresponding components of \mathbf{H} and also \mathbf{HPH}^T in Eq. (4c) of Part I become therefore small and the observations have only a weak impact on updating Vortex 3; the corresponding components of \mathbf{P} start growing until vortex interaction and increasingly efficient updates bring back the vortex to the region \mathcal{R} where the stations are located. Around $t \sim 100$, the EKF thus manages to bring back the estimated Vortex 3 close to the true state; shortly afterwards, however, it fails to correctly estimate Vortex 1 (Fig. 2(c) and (d)).

Note that, although the estimated vortex system does not represent well the true system, the velocity at the origin $(0, 0)$ is reasonably well reconstructed from the estimated system to fit the station observation (Fig. 2(g)). The estimated vortex system has thus reached a different state from the true system while providing a similar velocity field. This indicates the ill-posedness of the reconstruction of point-vortex positions from discrete velocities only. Regularization of this ill-posedness is provided by the cut-off criteria.

Fig. 3 illustrates a typical case of successful and efficient EKF performance using the Rankine-vortex method. After an initial adjustment interval of about 50 time units,

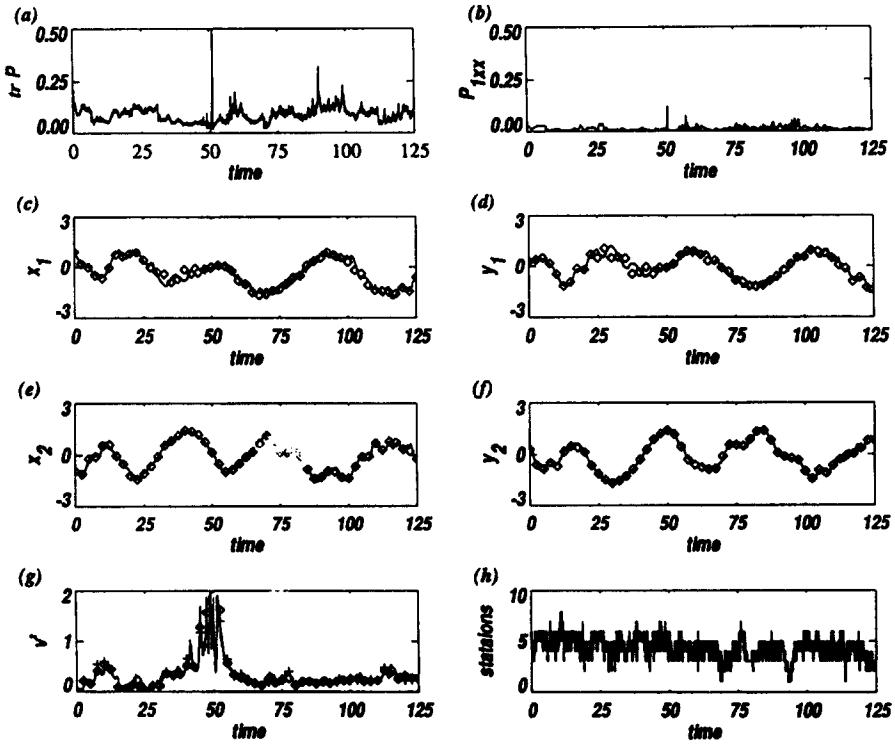


Fig. 3. The performance of the EKF for four Rankine vortices with stochastic forcing, when observing station velocities every 0.1 time units and a cut-off with $u_{\min} = 0.4$ is imposed: (a) trP ; (b) P_{1xx} ; (c) x_1 ; (d) y_1 ; (e) x_2 ; (f) y_2 ; (g) square of velocity at $(0, 0)$; and (h) number of active stations.

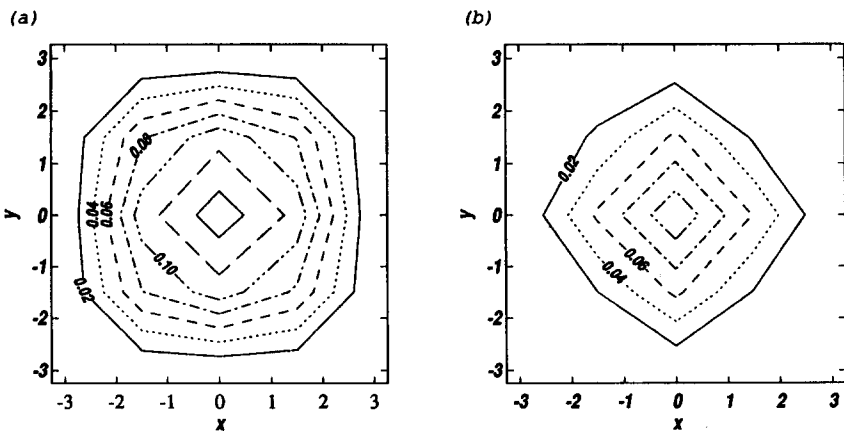


Fig. 4. Contour plots of: (a) number of times that a station has been used, and (b) probability density function of vortex population. Both plots are from a time series of 125 time units, and the former number is normalized by 1251, the total number of possible uses. Contour interval for both plots is 0.02.

during which the number of active stations is slightly higher, their number at each update time becomes, and stays, roughly the same as the number of vortices (Fig. 3(h)). Stations cover the area where both the estimated and the true vortex trajectories are, so that there are always some stations near each vortex to assure a proper update. Fig. 4(a) is a contour plot of the total number of times that each station has been used during 1251 updates, while Fig. 4(b) shows the probability density function (Silverman, 1986, Scott, 1992, Kimoto and Ghil, 1993a,b) of the true vortex population during the same time interval. Clearly, the stations in the neighborhood of the most likely vortex path are used often; the slight asymmetries in each one of the two plots, as well as the small difference between the two, are due to finite sampling and to the coarseness of the interpolation grid, with 25 grid points located at the same positions as the available observing stations.

Adding more available stations to any part of the region \mathcal{R} does not improve nor diminish the performance of the EKF for any ‘reasonable’ u_{\min} (not shown). Locating the available stations, however, far away from the area most heavily populated by the moving vortices leads to failure of the EKF (not shown).

On the other hand, the number of active stations is a very important factor in achieving successful tracking. For a given set of available stations, the number of active stations depends on the choice of u_{\min} . Increasing u_{\min} results in a decrease of the

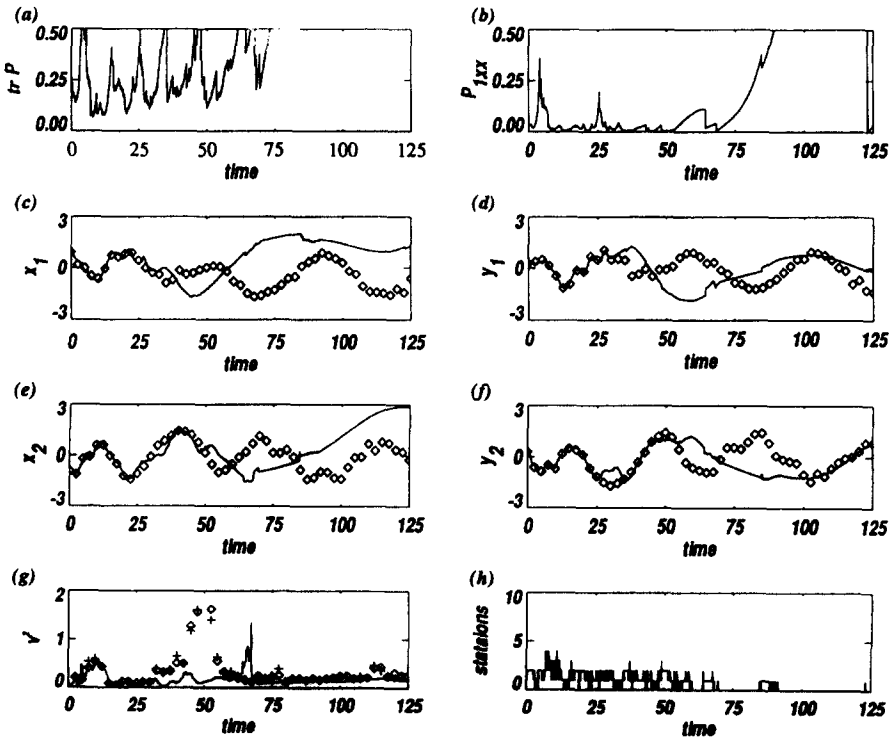


Fig. 5. Same as Fig. 3 but with a higher cut-off $u_{\min} = 0.53$.

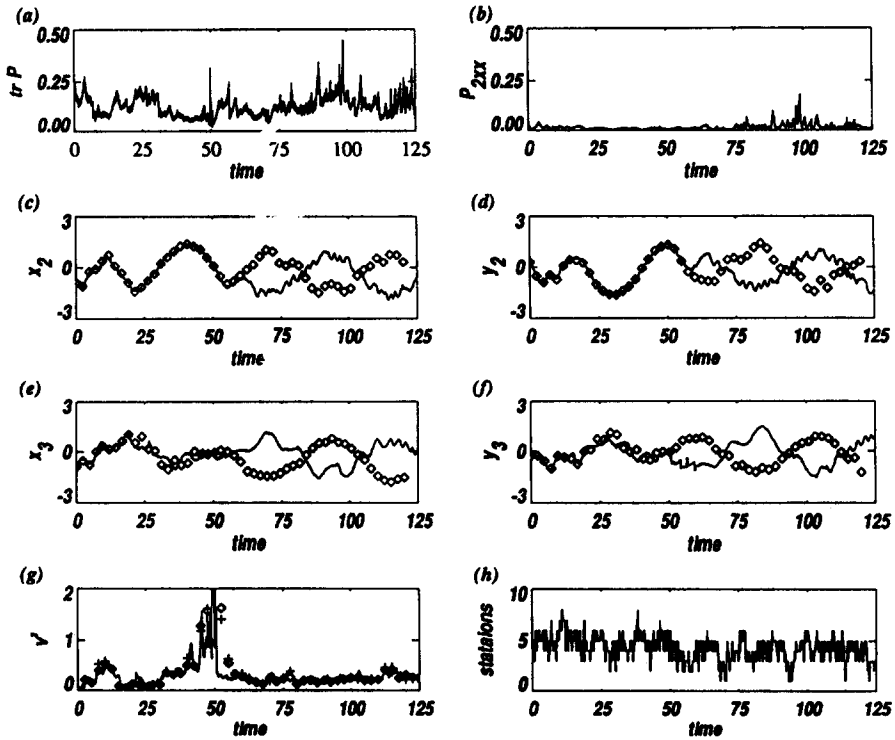


Fig. 6. Same as Fig. 3, but with a longer updating interval of 0.2 time units: (a) trP ; (b) P_{2xx} ; (c) x_2 ; (d) y_2 ; (e) x_3 ; (f) y_3 ; (g) square of velocity at $(0, 0)$; and (h) number of active stations.

number of active stations; for large enough u_{\min} , this decrease can lead to a situation where the number of observations is no longer sufficient to track the system, as shown in Fig. 5 where $u_{\min} = 0.53$. As when using the point-vortex method (Fig. 2), the components of P do pick up the signal of poor EKF performance (Fig. 5(a) and (b)); still, the active observations are too sparse to keep the estimated vortex system on track (Fig. 5(c)–(f)). Note that in this case, where the failure is due to insufficient observations, the estimated velocity can no longer follow the observed value (Fig. 5(g)).

Decreasing u_{\min} may also have a detrimental effect. Reducing u_{\min} by a relatively small amount ($u_{\min} \sim 0.3$) from the value of $u_{\min} = 0.4$ used in the successful tracking case of Fig. 3 increases the number of active stations, but EKF performance does not improve dramatically (not shown). By reducing u_{\min} too much ($u_{\min} < 0.1$), the system fails again due to the presence of excessively small velocity data; in fact by setting $u_{\min} = 0$, the EKF using Rankine vortices results in the same type of behavior as the EKF using point vortices (Fig. 2).

Observations that are not frequent enough may cause unsatisfactory performance of the EKF, like observations that are too sparse. In Fig. 6 appears an interesting case in which Vortices 2 and 3 switch their identities, i.e. after $t = 60$, the estimated Vortex 2 is tracking the true Vortex 3 and conversely (Fig. 6(c)–(f)). Without Lagrangian observa-

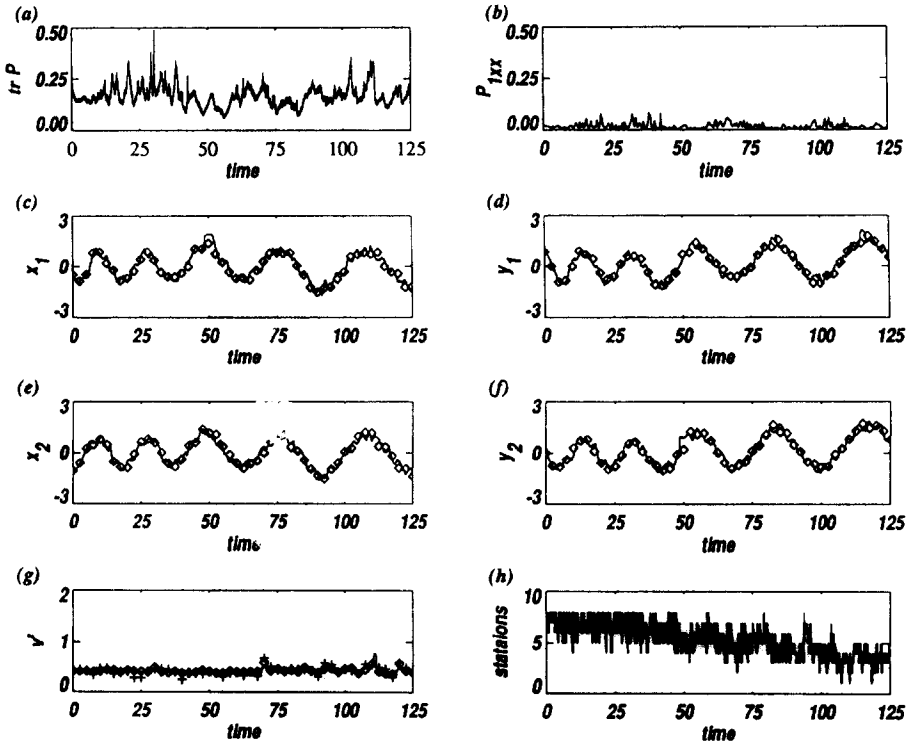


Fig. 7. Same as Fig. 5, but for six Rankine vortices and with $u_{\min} = 0.53$.

tions of the vortex position, the filter cannot recognize the switch, since the two vortices have the same circulation and are thus indistinguishable, based on either the components of \mathbf{P} or the reconstructed velocities.

Fig. 7 illustrates successful EKF performance for six Rankine vortices. The optimal cut-off threshold here is higher since the overall field velocities increase with the number of vortices of equal circulation. Although the vortex motion appears fairly simple from the time histories of the x - and y -positions shown in Fig. 7(c)–(f), the actual trajectories of the vortex centers are not. Fig. 8 shows the estimated and true trajectory of Vortex 1. Interestingly, the former exhibits less regularity than the latter: the EKF filters out the noise component of the system while capturing the essence of the deterministically chaotic motion.

As the number of vortices increases, so does the complexity of their dynamics. The basic mechanism of EKF performance, however, remains the same. After initial adjustment, the filter requires a number of active stations equal in the mean to the number of vortices at each update; this number only fluctuates by one to three stations, above or below the mean (Fig. 3(h)). The available stations cover homogeneously the whole area that the vortices tend to visit. The cut-off threshold u_{\min} needs to be selected judiciously, so that neither failure due to the small-velocity effect (u_{\min} too small) nor to the small number of active stations (u_{\min} too large) occur. Frequency of observation is

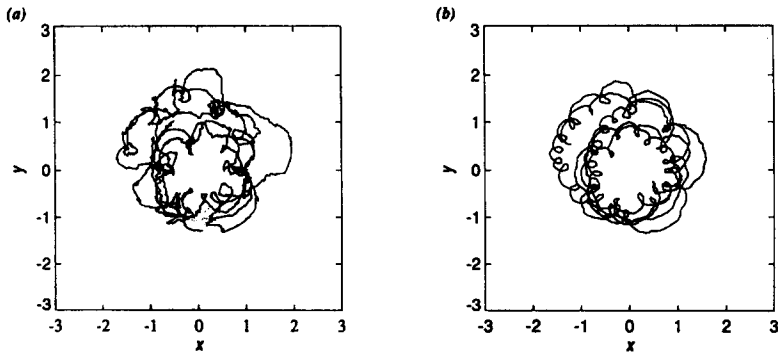


Fig. 8. Trajectory of Vortex 1 in Fig. 7: (a) estimated; and (b) true.

also an important factor. Due to the complex dynamics of the system, identity switching between the vortices may take place. This phenomenon is hard to prevent when all the vortices have equal circulations. It can be prevented either by observing at least one of the vortex positions or by introducing vortices with distinct circulations.

4. Observing-system optimization

In this section, we provide a simple analysis to help optimize the nonlinear Eulerian observing system, i.e. the distribution of available stations and active stations, the cut-off threshold u_{\min} , as well as the core radius of the Rankine vortices. We assume that all vortices have comparable total circulation Γ and core radius σ , and that they remain in a bounded domain of the plane throughout the assimilation, so as to contribute by observable velocity increments to the fixed-station measurements. Available stations are distributed over a rectangular grid in the plane.

We start with the estimation of the core radius. If any observations are available to give the core radius of isolated vortices, one should obviously use the estimate so obtained in formulating the model. However, if no observation is available, then the core radius σ_l of vortex l that will provide the best tracking can be chosen by one of the following two methods. The first method takes the statistical point of view: The true position of the centroid of concentrated vorticity associated with vortex l is most likely to lie within a circle of radius $\sqrt{P_{lxx}^2(0) + P_{lyy}^2(0)}$, where $P_{lxx}(0)$ and $P_{lyy}(0)$ are the components of the error-covariance matrix \mathbf{P} corresponding to the position of vortex l at the beginning of the data assimilation. Hence it is natural to approximate the true vorticity distribution within this circle by a Rankine vortex whose core radius is

$$\sigma_l = \sqrt{P_{lxx}^2(0) + P_{lyy}^2(0)}. \quad (3a)$$

The second method takes the dynamics of the flow into account. Since the Rankine-vortex approach was introduced to avoid the velocity singularity near a point vortex, it is natural to set a maximum velocity u_{\max} induced by a single vortex in the flow field. The

velocity around the Rankine vortex l (Fig. 1) increases linearly with distance r from the vortex center, achieves a maximum value of $\Gamma_l/2\pi\sigma_l$ at the core boundary, and then decays as $\Gamma_l/2\pi r$ outside the core, cf. Eq. (1); hence the core radius may be chosen as:

$$\sigma_l = \frac{\Gamma_l}{2\pi u_{\max}}. \quad (3b)$$

As discussed in the previous section, the optimal choice of the distribution of available and active stations, on the one hand, and the cut-off threshold u_{\min} , on the other, are closely related to each other. The optimal cut-off threshold u_{\min} is estimated first; we then determine the optimal distribution of available stations.

Since the velocity induced by a Rankine vortex decays relatively quickly outside its core, we only consider the contribution to the velocity field from the vortex which is closest to a given station in order to estimate u_{\min} . The obvious choice is to take the cut-off velocity as a given fraction of the maximum velocity at the core boundary:

$$u_{\min} = \frac{1}{2\pi\beta} \left(\frac{\Gamma}{\sigma} \right)_{\min}, \quad (4a)$$

where

$$\left(\frac{\Gamma}{\sigma} \right)_{\min} = \min \left\{ \frac{\Gamma_1}{\sigma_1}, \dots, \frac{\Gamma_N}{\sigma_N} \right\}. \quad (4b)$$

A reasonable range for the parameter β is $1 \leq \beta \leq 10$, to be able to eliminate small velocities, on the one hand, but not reduce the number of active stations too much, on the other. By this choice, any station within a circle of radius $\Gamma_l/2\pi u_{\min} \sim \beta\sigma_l$ from the center of vortex l is guaranteed to be an active station in the update of vortex positions.

For a Rankine-vortex system whose core radii were chosen based on the dynamical approach, i.e. Eq. (3b), u_{\min} and u_{\max} have the relation $u_{\max} = \beta u_{\min}$. To include the effect from additional vortices, β may be chosen slightly smaller for a system with a larger number of vortices because the total velocity is simply a linear superposition of the velocities induced by each vortex. The numerical and analytical arguments given here for station screening within the EKF application to Rankine-vortex systems are thus more solidly grounded in the dynamics of the assimilation process than the screening of observations in operational OI; the latter is largely a matter of meeting computational restrictions, based purely on empirical and statistical considerations.

Estimation of the optimal available station distribution needs to take the global flow dynamics into account. There are three conditions: First of all, if the vortices are sparsely distributed, then each vortex, l say, should have at least one active station within the circle of radius $\Gamma_l/2\pi u_{\min}$ from its center for the individual update of that vortex's center position to be efficient. Hence the optimal distance r_G between two stations in this case is

$$r_G = \frac{2\Gamma_{\min}}{\beta} \left/ \left(\frac{\Gamma}{\sigma} \right)_{\min} \right., \quad (5a)$$

where

$$\Gamma_{\min} = \min\{\Gamma_1, \dots, \Gamma_N\}. \quad (5b)$$

On the other hand, if N vortices co-exist in a relatively small area then all of them, rather than a single one, have significant impact on the total velocity measured at an active station, so that one should take the spacing between stations as

$$r_G = \frac{2N\Gamma_{\min}}{\beta} \left/ \left(\frac{\Gamma}{\sigma} \right)_{\min} \right. . \quad (5c)$$

Furthermore, the available stations should be placed so that at least a number of stations equal to that of vortices exist in the region where the vortices spend most of the time. If the available stations were more densely distributed than the estimate above, the EKF with the proper choice of u_{\min} would most likely increase the number of active stations but the overall performance would not improve significantly, as shown numerically in the previous section.

In the present numerical study, all core radii were chosen as $\sigma = 0.1$, which is comparable with $\sqrt{P_{xx}^2(0) + P_{yy}^2(0)}$. The cut-off threshold u_{\min} was chosen based on $\beta = 4$ in Figs. 3 and 6 for four-vortex systems, and on $\beta = 3$ in Figs. 5 and 7 for four- and six-vortex systems, respectively. The station spacing r_G was set to 1.5 to meet the criterion Eq. (5c) for the available-station distribution.

5. Summary and discussion

The extended Kalman filter (EKF) was used in Part II of this study to estimate flow fields whose dynamics is described by a Lagrangian representation (i.e. by vortex methods) using Eulerian observations (such as station velocities) in the presence of stochastic forcing. In Part I of the study (Ide and Ghil, 1997a), the dynamics was represented by a point-vortex system and it was shown that the EKF with Lagrangian observations of vortex position solely or in combination with velocity observations, can provide excellent tracking as long as stochastic forcing is taken into account. The sole use of Eulerian observations, on the other hand, may be unsuccessful in a point-vortex system, due to one of two causes: velocity measured being too large, because of the singular velocity profile of point vortices and their immediate proximity to a station, or too small because of cancellation between large contributions from some vortices or the remoteness from all vortices.

To overcome the former problem, the Rankine-vortex method was introduced in the present Part II. This is the next step in a hierarchy of approximations of localized vorticity concentrations: the dynamics is still described by the motion of the centers of the vortex cores, governed by the same equations as the corresponding point vortices with the same circulation; the vortex configuration, i.e. the radius of the core in solid-body rotation, is kept fixed, thus removing the velocity singularity of the point vortices. The latter problem is addressed by imposing a cut-off criterion with threshold u_{\min} to eliminate the use of small-velocity data in the updating process.

Numerical experiments show successful tracking of deterministically chaotic, four- and six-vortex systems when using velocity data only. The EKF performs well for judiciously chosen observing-system parameters but may fail when improper criteria are selected. The error-covariance matrix does exhibit, however, the signs of unsuccessful tracking in most cases.

The key elements of successful EKF performance for a Rankine-vortex system are: the distribution of available stations, the criteria for station selection at each update, and the frequency of observations. Simple analysis provides optimal estimates for these key elements, together with the optimal size of the Rankine vortex cores. Our analytical estimates are supported by the numerical results. The available stations should cover homogeneously the whole area where the vortices evolve over the time interval of interest, and their optimal spacing can also be determined.

As the number of vortices increases, the complexity of their dynamics also increases. The basic mechanisms of EKF performance, however, remain the same. Successful tracking still requires roughly the same number of active stations in each update as there are vortices.

Work in progress addresses EKF performance for the next step in our hierarchy of approximations for vorticity concentrations, namely elliptical vortices (Kida, 1981, Melender et al., 1987, Ide and Wiggins, 1995). In this case, centroid position as well as ellipticity and attitude angle of the ellipse of uniform vorticity have to be estimated (Ide and Ghil, 1997c).

Acknowledgements

One of us (MG) has learned from Richard L. Pfeffer about the diagnostics of laboratory experiments, with many (Li et al., 1986) or fewer (Bernardet et al., 1990) probes available: we hope that the EKF will permit better tracking of laboratory experiments in the latter case as well. It is a pleasure to thank J.C. McWilliams and S. Wiggins for many interesting discussions on vortex dynamics. The presentation was greatly improved by detailed comments from R. Daley and three anonymous reviewers. This work was supported by NSF Grant ATM90-13217 (KI), ONR Grant N0014-89-J-1845 (KI and MG), NASA Grant NAG-5713 (KI and MG) and by a Professorship of the Académie des Sciences, Paris, held at the Ecole Normale Supérieure, Paris (MG). This is IGPP contribution no. 4604.

References

- Aref, H., 1984. Integrable, chaotic, and turbulent vortex motion in two-dimensional flow. *Ann. Rev. Fluid Mech.* 15, 345–389.
- Barth, N., 1992. Oceanographic experiment design II: Generic algorithms. *J. Atmos. Ocean. Tech.* 9, 434–443.
- Barth, N., Wunsch, C., 1990. Oceanographic experiment design by simulated annealing. *J. Phys. Oceanogr.* 20, 1249–1263.
- Bengtsson, L., Ghil, M., Källén, E. (Eds.), 1981. *Dynamic Meteorology: Data Assimilation Methods*, Appl. Math. Sci. Ser. vol. 36. Springer-Verlag, 330 pp.

- Bennett, A.F., 1992. *Inverse Methods in Physical Oceanography*. Cambridge University Press, 346 pp.
- Bernardet, P., Butet, A., Déqué, M., Ghil, M., Pfeffer, R.L., 1990. Low-frequency oscillation in a rotating annulus with topography. *J. Atmos. Sci.* 47, 3007–3022.
- Carter, E.F., 1989. Assimilation of Lagrangian data into a numerical model. *Dyn. Atmos. Oceans* 13, 348–355.
- Daley, R., 1991. *Atmospheric Data Analysis*. Cambridge University Press, 420 pp.
- Feliks, Y., Ghil, M., 1996. Mixed barotropic–baroclinic eddies on an eastward midlatitude jet. *Geophys. Astrophys. Fluid Dyn.* 84, 165–204.
- Gelb, A. (Ed.), 1974. *Applied Optimal Estimation*. The MIT Press, 374 pp.
- Ghil, M., 1989. Meteorological data assimilation for oceanographers. Part I: Description and theoretical framework. *Dyn. Atmos. Oceans* 13, 171–218.
- Ghil, M., Ide, K., 1994. Extended Kalman filtering for vortex systems: an example of observing system design. In: Brasseur, P., Nihoul, J.C.J. (Eds.), *Data Assimilation for Modelling the Ocean in a Global Change Perspective*. Springer-Verlag, New York, pp. 107–193.
- Ghil, M., Malanotte-Rizzoli, P., 1991. Data assimilation in meteorology and oceanography. *Adv. Geophys.* 33, 141–226.
- Ghil, M., Solan, A., 1973. Heat transfer through a Rankine vortex. *J. Heat Transfer* 33, 137–139.
- Ghil, M., Cohn, S.E., Tavantzis, J., Bube, K., Isaacson, E., 1981. Application of estimation theory to numerical weather prediction. In: Bengtsson, L., Ghil, M., Källén, E. (Eds.), *Dynamic Meteorology: Data Assimilation Methods*. Appl. Math. Sci. Ser. vol. 36. Springer-Verlag, pp. 139–224.
- Ide, K., Ghil, M., 1995. An analytical study of geophysical flow estimation and mixing using extended Kalman filtering for vortex systems. In: *Proceedings of the Second WMO International Symposium on Assimilation of Observations in Meteorology and Oceanography*, Tokyo, vol. 1. pp. 159–164.
- Ide, K., Ghil, M., 1997a. Extended Kalman filtering for vortex systems. Part I: Methodology and point vortices. *Dyn. Atmos. Oceans* 27, 301–332.
- Ide, K., Ghil, M., 1997b. Evolution of prediction errors in nonlinear systems, deterministic and stochastic. (In preparation.)
- Ide, K., Ghil, M., 1997c. Extended Kalman filtering for elliptical vortices. (In preparation.)
- Ide, K., Wiggins, S., 1995. The dynamics of elliptically shaped regions of uniform vorticity in time-dependent linear external velocity fields. *Fluid Dyn. Rev.* 15, 205–235.
- Ide, K., Courtier, D., Ghil, M., Lorenc, A., 1997. Unified notation for data assimilation: Operational Sequential and Variational. *J. Meteor. Soc. Jpn.* 75, 181–189.
- Jazwinski, A.H., 1970. *Stochastic Processes and Filtering Theory*. Academic Press, 376 pp.
- Kalman, R.E., 1960. A new approach to linear filtering and prediction problems. *Trans. ASME, Ser. D, J. Basic Eng.* 82D, 35–45.
- Kalman, R.E., Bucy, R.S., 1961. New results in linear filtering and prediction problems. *Trans. ASME, Ser. D, J. Basic Eng.* 83D, 95–108.
- Kida, S., 1981. Motion of an elliptical vortex in a uniform shear flow. *J. Phys. Soc. Jpn.* 50 (10), 3517–3520.
- Kimoto, M., Ghil, M., 1993a. Multiple flow regimes in the Northern Hemisphere winter. Part I: Methodology and hemispheric regimes. *J. Atmos. Sci.* 50, 2625–2643.
- Kimoto, M., Ghil, M., 1993b. Multiple flow regimes in the Northern Hemisphere winter. Part II: Sectorial regimes and preferred transitions. *J. Atmos. Sci.* 50, 2645–2673.
- Li, G.Q., Pfeffer, P.L., Kung, R., 1986. An experimental study of baroclinic flows with and without two-wave bottom topography. *J. Atmos. Sci.* 43, 2585–2599.
- Mariano, A.J., 1990. Contour analysis: a new approach for melding geophysical fields. *J. Atmos. Ocean. Tech.* 7, 285–295.
- McWilliams, J.C., 1980. An application of equivalent modons to atmospheric blocking. *Dyn. Atmos. Oceans* 5, 43–66.
- McWilliams, J.C., 1991. Geostrophic vortices. In: Osborne, A.R. (Ed.), *Nonlinear Topics in Ocean Physics: Proceedings of the International School of Physics “Enrico Fermi” Course 109*. North-Holland, Elsevier Science Publishers B.V., Amsterdam, pp. 5–50.
- Melender, M.Y., Zabusky, N.J., Styczek, S., 1987. A moment model for vortex interactions of the two-dimensional Euler equations. Part I: Computation of a Hamiltonian elliptical representation. *J. Fluid Mech.* 167, 95–115.

- Miller, R., Ghil, M., Gauthiez, F., 1994. Advanced data assimilation in strongly non-linear dynamical systems. *J. Atmos. Sci.* 51, 1037–1056.
- Olson, D.B., 1980. The physical oceanography of two rings observed by the cyclonic ring experiment. Part II: Dynamics. *J. Phys. Oceanogr.* 10, 514–528.
- Panel on Model-Assimilated Data Sets for Atmospheric and Oceanic Research, 1991. *Four-Dimensional Model Assimilation of Data: A Strategy for the Earth System Sciences*. National Academy Press, 78 pp.
- Robinson, A.R. (Ed.), 1983. *Eddies in Marine Science*. Springer-Verlag, 609 pp.
- Robinson, A.R., Spall, M.A., Walstad, L.J., Leslie, W.G., 1989. Data assimilation and dynamical interpolation in gulfcast experiments. *Dyn. Atmos. Oceans* 13, 301–316.
- Scott, D.W., 1992. *Multivariate Density Estimation*. Wiley-Interscience, 317 pp.
- Silverman, B.W., 1986. *Density Estimation for Statistics and Data Analysis*. Chapman and Hall, 175 pp.
- Wunsch, C., 1988. Transient tracers as a problem in control theory. *J. Geophys. Res.* 93, 8099–8110.